

# **Numerical Modelling of a Cascadia Subduction Zone Tsunami at the Canadian Coast Guard Base in Seal Cove, Prince Rupert, British Columbia**

Isaac V. Fine, Richard E. Thomson, Lauren M. Lupton and Stephen Mundschutz

Ocean Sciences Division  
Fisheries and Oceans Canada  
Institute of Ocean Sciences  
9860 West Saanich Road  
Sidney, BC  
V8L 4B2

2018

**Canadian Technical Report of  
Hydrography and Ocean Sciences 322**



Fisheries and Oceans  
Canada

Pêches et Océans  
Canada

Canada

## **Canadian Technical Report of Hydrography and Ocean Sciences**

Technical reports contain scientific and technical information of a type that represents a contribution to existing knowledge but which is not normally found in the primary literature. The subject matter is generally related to programs and interests of the Oceans and Science sectors of Fisheries and Oceans Canada.

Technical reports may be cited as full publications. The correct citation appears above the abstract of each report. Each report is abstracted in the data base *Aquatic Sciences and Fisheries Abstracts*.

Technical reports are produced regionally but are numbered nationally. Requests for individual reports will be filled by the issuing establishment listed on the front cover and title page.

Regional and headquarters establishments of Ocean Science and Surveys ceased publication of their various report series as of December 1981. A complete listing of these publications and the last number issued under each title are published in the *Canadian Journal of Fisheries and Aquatic Sciences*, Volume 38: Index to Publications 1981. The current series began with Report Number 1 in January 1982.

## **Rapport technique canadien sur l'hydrographie et les sciences océaniques**

Les rapports techniques contiennent des renseignements scientifiques et techniques qui constituent une contribution aux connaissances actuelles mais que l'on ne trouve pas normalement dans les revues scientifiques. Le sujet est généralement rattaché aux programmes et intérêts des secteurs des Océans et des Sciences de Pêches et Océans Canada.

Les rapports techniques peuvent être cités comme des publications à part entière. Le titre exact figure au-dessus du résumé de chaque rapport. Les rapports techniques sont résumés dans la base de données Résumés des sciences aquatiques et halieutiques.

Les rapports techniques sont produits à l'échelon régional, mais numérotés à l'échelon national. Les demandes de rapports seront satisfaites par l'établissement auteur dont le nom figure sur la couverture et la page de titre.

Les établissements de l'ancien secteur des Sciences et Levés océaniques dans les régions et à l'administration centrale ont cessé de publier leurs diverses séries de rapports en décembre 1981. Vous trouverez dans l'index des publications du volume 38 du Journal canadien des sciences halieutiques et aquatiques, la liste de ces publications ainsi que le dernier numéro paru dans chaque catégorie. La nouvelle série a commencé avec la publication du rapport numéro 1 en janvier 1982.

Canadian Technical Report of  
Hydrography and Ocean Sciences 322

2018

NUMERICAL MODELLING OF A CASCADIA SUBDUCTION ZONE TSUNAMI  
AT THE CANADIAN COAST GUARD BASE IN SEAL COVE, PRINCE RUPERT,  
BRITISH COLUMBIA

by

Isaac V. Fine, Richard E. Thomson, Lauren M. Lupton and Stephen Mundschutz

Ocean Sciences Division  
Fisheries and Oceans Canada  
Institute of Ocean Sciences  
9860 West Saanich Road  
Sidney, BC, V8L

© Her Majesty the Queen in Right of Canada, 2018.

Cat. No. Fs97-18/322E-PDF ISBN 978-0-660-25113-4 ISSN 1488-5417

Correct citation for this publication:

Isaac V. Fine, Richard E. Thomson, Lauren M. Lupton and Stephen Mundschutz, 2018. Numerical Modelling of a Cascadia Subduction Zone Tsunami at the Canadian Coast Guard Base in Seal Cove, Prince Rupert, British Columbia. Can. Tech. Rep. Hydrogr. Ocean Sci. 322: v + 34p.



## CONTENTS

1	CASCADIA SUBDUCTION ZONE EARTHQUAKES AND TSUNAMI.....	1
2	NUMERICAL SIMULATION OF A CASCADIA SUBDUCTION ZONE TSUNAMI .....	3
2.1	Model Setup: Nested Grid Formulation .....	3
2.1.1	Coarse Grid (Grid 1) .....	4
2.1.2	Intermediate Grid (Grid 2) .....	6
2.1.3	Intermediate Grid (Grid 3) .....	8
2.1.4	Final Grid (Grid 4) .....	9
2.2	Model Reference Levels.....	10
2.3	Cascadia Subduction Zone Tsunami Source Distributions .....	10
3	RESULTS .....	13
3.1	Comparison of Modelled Tsunami Waves for Two Cascadia Subduction Zone Scenarios for Coarse and Intermediate Grids .....	13
3.2	Detailed Results for Seal Cove: Variations in Sea Level and Tsunami- Induced Currents .....	17
4	CONCLUSIONS .....	29
5	ACKNOWLEDGEMENTS .....	31
6	REFERENCES .....	33

## ABSTRACT

### **Numerical Modelling of a Cascadia Subduction Zone Tsunami at the Canadian Coast Guard Base in Seal Cove, Prince Rupert, British Columbia**

Isaac V. Fine, Richard E. Thomson, Lauren M. Lupton and Stephen Mundschutz 2018. Numerical Modelling of a Cascadia Subduction Zone Tsunami at the Canadian Coast Guard Base in Seal Cove, Prince Rupert, British Columbia. Tech. Rep. Hydrogr. Ocean Sci. 322: v + 34p.

The last major megathrust earthquake along the Cascadia Subduction Zone (CSZ) off the west coast of North America occurred in January 1700. The massive tsunami waves generated by this moment magnitude ( $M_w$ ) 9.0 event caused significant destruction as far away as Japan on the opposite side of the Pacific Ocean. Future CSZ events pose a high risk for destructive tsunamis along the British Columbia coast.

This work uses a nested-grid numerical tsunami model to predict the tsunami waves and currents at Sea Cove near Prince Rupert generated by an  $M_w$  9.0 CSZ failure. Two updated earthquake source models are used: A buried rupture model (A) and a splay-fracture model (B). Both models include new source areas to the west of Vancouver Island. The analysis is in anticipation of upgrades and modernization of the Canadian Coast Guard facility at Seal Cove.

Tsunami waves at the Coast Guard base predicted by the buried rupture Model A were highest, reaching an amplitude of 0.76 m above the tidal level, compared to 0.65 m for Model B. The 6<sup>th</sup> wave is the highest. Predicted wave-induced currents within Seal Cove are weak but reach speeds of around 2.0 m/s (4 knots) in adjacent Fern Passage. Incorporation of a 50% safety factor indicates that the safe water level for Seal Cove should be at least 1.14 m above Mean Higher High Water, or 3.45 m above Mean Sea Level.

## RESUME

### **Modélisation numérique d'un tsunami à proximité de la zone de subduction de Cascadia à la base de la Garde côtière canadienne de Seal Cove, à Prince Rupert, Colombie-Britannique**

Isaac V. Fine, Richard E. Thomson, Lauren M. Lupton and Stephen Mundschutz 2018. Numerical Modelling of a Cascadia Subduction Zone Tsunami at the Canadian Coast Guard Base in Seal Cove, Prince Rupert, British Columbia. Tech. Rep. Hydrogr. Ocean Sci. 322: v + 34p.

Le dernier mégaséisme majeur le long de la zone de subduction de Cascadia (ZSC) au large de la côte ouest de l'Amérique du Nord est survenu en janvier 1700. Les vagues sismiques océaniques générées par ce séisme de 9,0 sur l'échelle de magnitude de moment ( $M_w$ ) ont causé des dégâts considérables, aussi loin que le Japon, de l'autre côté de l'océan Pacifique. L'activité sismique potentielle future le long de la ZSC pose un risque élevé de tsunamis destructeurs sur la côte de la Colombie-Britannique.

Ce projet utilise un modèle numérique à grille à maille variable afin de prédire les ondes de tsunamis et les courants à Seal Cove, près de Prince Rupert, en cas de séisme de 9,0  $M_w$  le long de la ZSC. Deux modèles de source des séismes sont employés : le modèle de fracture enfouie (A) et un modèle de fracture de la faille subsidiaire d'amortissement (B). Les deux modèles comprennent de nouvelles zones sources à l'ouest de l'île de Vancouver. L'analyse est effectuée en vue des futures mises à niveau et de la modernisation de l'installation de la Garde côtière à Seal Cove.

Les ondes de tsunamis qui frapperaient le site de la Garde côtière selon le modèle de fracture enfouie (modèle A) sont les plus hautes, atteignant une amplitude de 0,76 m au-dessus du niveau de la marée, contre 0,65 m pour le modèle B. La sixième vague est la plus haute. À Seal Cove, les courants engendrés par les vagues ne seraient pas très puissants, mais atteindraient des vitesses d'environ 2,0 m/s (4 nœuds) dans le passage Fern adjacent. L'application d'un coefficient de sécurité de 50 % indique que le niveau d'eau sécuritaire de Seal Cove devrait se trouver au moins à 1,14 m au-dessus de la moyenne des pleines mers supérieures, ou 3,45 m au-dessus du niveau moyen de la mer.



Photo of Seal Cove, BC, traveller of Ocean Pacific Air to tripadvisor.ca

## 1 CASCADIA SUBDUCTION ZONE EARTHQUAKES AND TSUNAMI

Cascadia Subduction Zone (CSZ) tsunamis are the main tsunami threat for the west coast of British Columbia (Clague et al., 2003; Leonard et al., 2014). The Great CSZ earthquake of 26 January 1700 (moment magnitude,  $M_w = 9.0$ ) generated a major trans-oceanic tsunami that caused significant destruction in Japan and strongly affected the west coasts of the USA and Canada. Results from recent paleotsunami studies along the coast of Vancouver Island and the west coast of the USA (cf. Clague, 2000), and preliminary numerical modelling of CSZ tsunamis for coastal North America (cf. Cherniawsky et al., 2007; Fine et al., 2008; Cheung et al., 2011, AECOM, 2013), demonstrate the high risk of CSZ tsunamis for British Columbia. Numerous seismotectonic studies indicate that great megathrust earthquakes in the CSZ region have occurred on a regular basis in the past and can be expected to occur with an average return period of about 500 years in the foreseeable future (Witter et al., 2013; Wang and Tréhu, 2016).

The 1100 km long CSZ extends from Cape Mendocino in northern California to central Vancouver Island (Figure 2.1). Subduction of the Pacific Plate beneath the North American Plate takes place about 100 km to the west of Vancouver Island. Given the relatively long seismic quiescence, this region is now considered under high risk from a major megathrust earthquake and consequent tsunami that could strike the southwest coast of British Columbia (Dragert and Rogers, 1988). As part of natural hazard risk mitigation studies, several investigators have undertaken numerical computations of potential tsunamis originating from a megathrust CSZ failure along the North America coast (e.g., Ng et al., 1990, 1991; Whitmore, 1993). Investigations of CSZ tsunamis dramatically increased following reliable evidence of a Mw 9.0 megathrust earthquake and associated great trans-Pacific tsunami on 26 January 1700 that swept along the nearly 1000-km Pacific coast of Japan and led to intense flooding along the California, Oregon, Washington and Vancouver Island coasts (Atwater et al., 1995; Satake et al., 1996).

This report presents modelled results from numerically simulated tsunami waves representative of CSZ earthquakes of Mw = 9.0. Focus is on estimating the magnitude and arrival times for expected tsunami waves for the Canadian Coast Guard Base at Seal Cove in Prince Rupert, British Columbia. This research is part of a larger study to inform future redesigns of Canadian Coast Guard stations to mitigate the impact on the operability at these stations in the event of a major CSZ earthquake.

Initial studies showed that tsunamis generated by a Mw ~9.0 CSZ earthquake could present a major threat to the west coast of the United States and southwest coast of British Columbia. The estimated wave runup for the January 1700 Cascadia tsunami along the west coastlines of North America was up to 20 m (Atwater et al., 1995). Further numerical studies were undertaken to estimate possible tsunami risk for settlements along the outer, west coast of Vancouver Island associated with such earthquakes (cf. Myers et al., 1999; Cherniawsky et al., 2007; Fine et al., 2008; Cheung et al., 2011). These studies used source models that reflected the current science at the time of the respective study. Detailed characterization of megathrust rupture models used for simulating tsunami inundation was presented by Witter et al. (2013). The authors examined 15 megathrust earthquake scenarios, looking in detail at three main scenarios.

The splay-fault rupture referred to as Model 1 (M1) is of particular interest for the present study as it represents the most likely case based on present information. For this model, Witter et al. (2013) used an extremely high resolution numerical mesh to allow accurate modelling of the surface-breaching rupture. As stated by Witter et al. (2013), the model has the following parameters: Length = 1000 km; width = 83 km; maximum slip = 18 m; average slip = 9 m; seismic moment =  $2.9 \cdot 10^{22}$  N·m; and Mw = 8.9. This work uses a slightly modified version of the model according to the recommendations of Wang and Tréhu (2016) to simulate the tsunami risk for Seal Cove (Prince Rupert Harbour area).

## 2 NUMERICAL SIMULATION OF A CASCADIA SUBDUCTION ZONE TSUNAMI

### 2.1 MODEL SETUP: NESTED GRID FORMULATION

Accurate numerical simulation of tsunami waves in the rapidly shoaling regions of the west coast of British Columbia requires setting up a model domain as a series of nested grids of ever finer spatial and temporal resolution. The use of nested grids of smaller cell dimensions and time steps makes it possible to resolve tsunami wave configurations as they propagate into the shallow coastal regions. The principal requirements for numerical models using nested grids are as follows:

- Nested grid cell sizes are generally obtained by dividing the initial, large-scale coarse numerical grid by an integer, typically 3 to 5. Integers larger than this can lead to grid interface problems;
- Nested grids are needed in near-coastal areas; the coarse “parent” grid should be of sufficient extent to resolve possible feed-back effects that the nested grid may have on the parent grid during the simulation time;
- A good interface between the inner and outer domains is required to avoid errors and model instability associated with point matching between the different grids. This should allow two-way fluxes without trapping shorter waves at the inner domain boundaries;
- High resolution bathymetry, external forcing and observations are needed for model domain setup, initialization and validation at each domain level; here the nested-grid formulation is similar to that used in well-known tsunami models, TUNAMI and COMCOT (Liu *et al.*, 1998; Imamura, *et al.*, 2006; Wang, 2009).

Dispersion effects can be included in the model by substituting numerical dispersion for the actual physical dispersion. Solving this issue (see for example, Imamura *et al.*, 1988) has made it possible for investigators to cover large, open ocean regions, representative of an area affected by a CSZ tsunami, using a relatively coarse grid with a cell size of roughly 10 km by 10 km (4-5 arc-seconds).

Because of the relatively long periods of the tsunamis generated in the deep-water source regions used in this study, and because of the relatively short propagation times of 3 to 4 hours between the source region and the Seal Cove site, the dispersion effect is negligible. In this case, high bathymetric resolution is the important factor for modelling wave propagation in the offshore regions.

The present project uses a series of four nested grids for the CSZ tsunami model (Table 1). The choice of model grids takes into account the need for high spatial resolution to accurately resolve the reflection and transformation of the waves and the need for a sufficiently large spatial extent to capture the effects of frequency dispersion during long distance wave propagation.

Table 1. Parameters of the numerical grids used in the CSZ tsunami generation and propagation model. Grid extent is along the x (eastward) and y (northward) coordinate directions and is presented in degrees (°). Numerical grid cell sizes for Grids 2, 3 and 4 are roughly 270, 54 and 11 m, respectively. CHS refers to the Canadian Hydrographic Service.

<b>Grid No.</b>	<b>Extent (x, y) (degrees)</b>	<b>Array (number of grid points)</b>	<b>Cell size (x, y) (degrees)</b>	<b>Source of data</b>	<b>Processing type</b>
<b>1</b>	28.0, 24.0	1121, 1921	0.025, 0.0125	GEBCO 2014 30 arc- seconds gridded data	Filtering and bilinear interpolation
<b>2</b>	5.0, 6.2	1201, 2480	0.00416667, 0.0025	BC Coastal Relief, 3 sec, Southern Alaska Coastal Relief 8 sec	Filtering and bilinear interpolation
<b>3</b>	1.0086, 0.526	1339, 1053	0.0008333, 0.0005	CHS bathymetry data	Filtering and bilinear interpolation
<b>4</b>	0.13, 0.06	781, 701	0.000166667, 0.0000833	CHS bathymetry data	Kriging, smoothing, bilinear interpolation

### **2.1.1 Coarse Grid (Grid 1)**

Grid 1 is the outer domain and covers the northeast Pacific, encompassing the major source region used in the simulations, the CSZ (Figure 2.1). We note that the northeast Pacific is an important tsunami wave generation region through which all offshore tsunamis propagate on their way to the British Columbia coast. The spatial resolution of the coarse grid is 90 arc-seconds in the east-west direction (spatial scales in x range from 1.4 km to 2.2 km, depending on latitude) and 45 arc-seconds in the north-south direction (1.4 km grid size in the y-direction). The grid is bounded by 38– 62° N, 150 – 122° W and was created using the 30 arc-second global bathymetry dataset GEBCO (Becker et al., 2009).

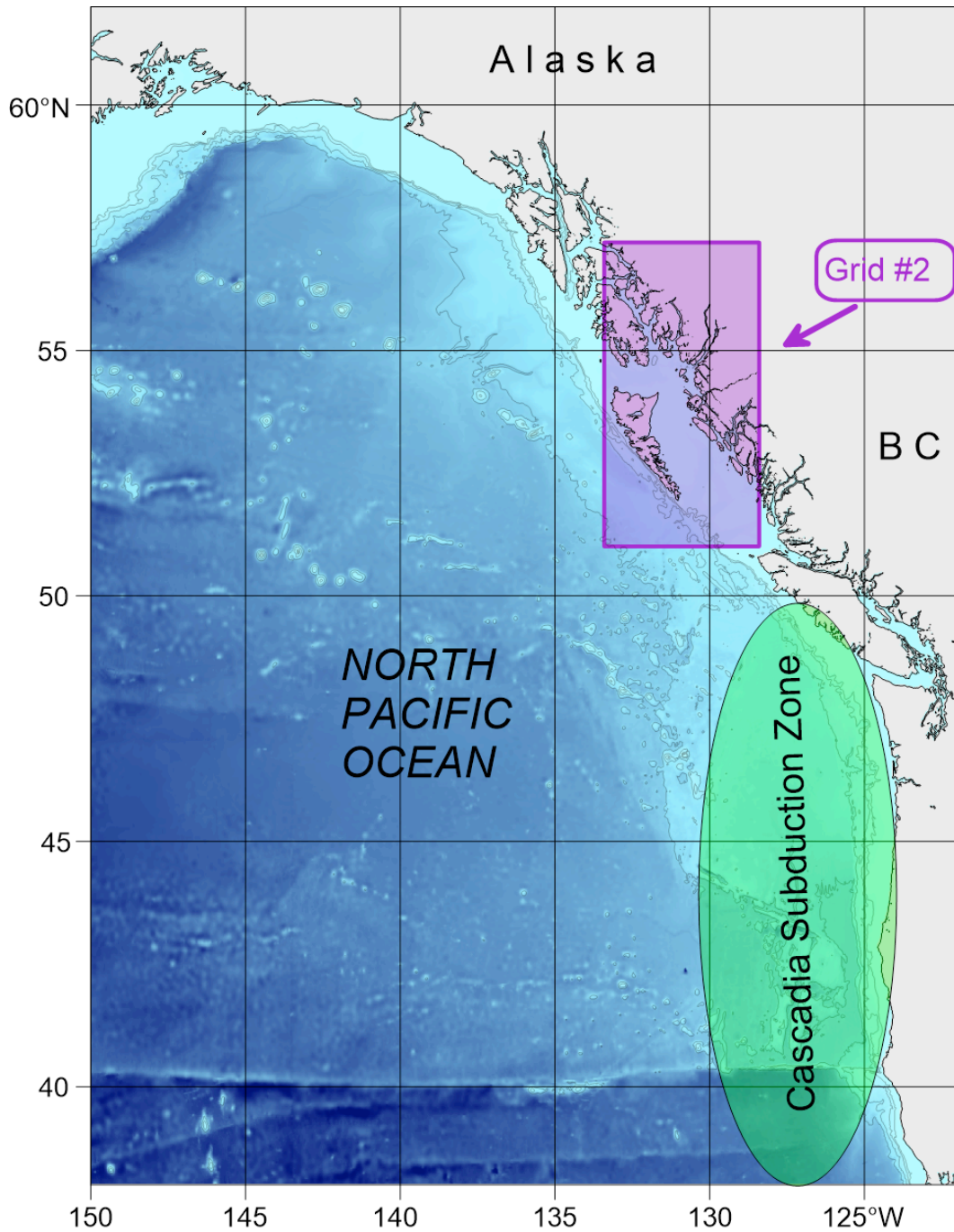


Figure 2.1. The region covered by the large-scale coarse grid numerical model for the northeast Pacific (Grid 1). Also shown is the CSZ where a tsunami could be generated that would impact the Coast Guard facility. The insert shows the location of the first nested grid (Grid 2), covering the northwest coast of British Columbia.



### **2.1.2 Intermediate Grid (Grid 2)**

Grid 2 covers northwest British Columbia and southeast Alaska (Figure 2.2). The location and coverage of the grid was chosen so that it extends equally to the north and to the south of the Prince Rupert region. This intermediate grid enables simulation of wave shoaling and wave transformation as the tsunami propagates from the deep ocean to the shelf and into coastal areas. The grid is also important for energy exchange between different parts of the coast and shelf areas.

The southern part of the grid was created using the British Columbia 3 arc-second Digital Elevation Model (NOAA, 2017); the northern part was created using the 8 arc-second Southern Alaska Coastal Relief (Candwell et al., 2012). The British Columbia coastal relief map stops at 54.20°N at its northern boundary and it does not include the Prince Rupert area. In contrast, the Alaska topographic relief map extends to 19°N and includes the Prince Rupert area, but does not have sufficient accuracy for the Canadian region and were excluded where the grid crossed into Canadian waters.

The excluded data were replaced with available Canadian Hydrographic Survey (CHS) data. Thus, the northern boundary between the datasets was at around 54.5°N in the northern part of Dixon Entrance. To ensure there were no discontinuities between the two datasets, a smooth transition zone was inserted between them. Grid 2 has a resolution of 15 arc-seconds in the east-west direction and 9 arc-seconds in the north-south direction. This corresponds to grid cell spatial scales of approximately 270 m by 280 m, respectively (Table 1). The grid spans the northern coast with boundaries of 51°–57°N, 134°–128°W.

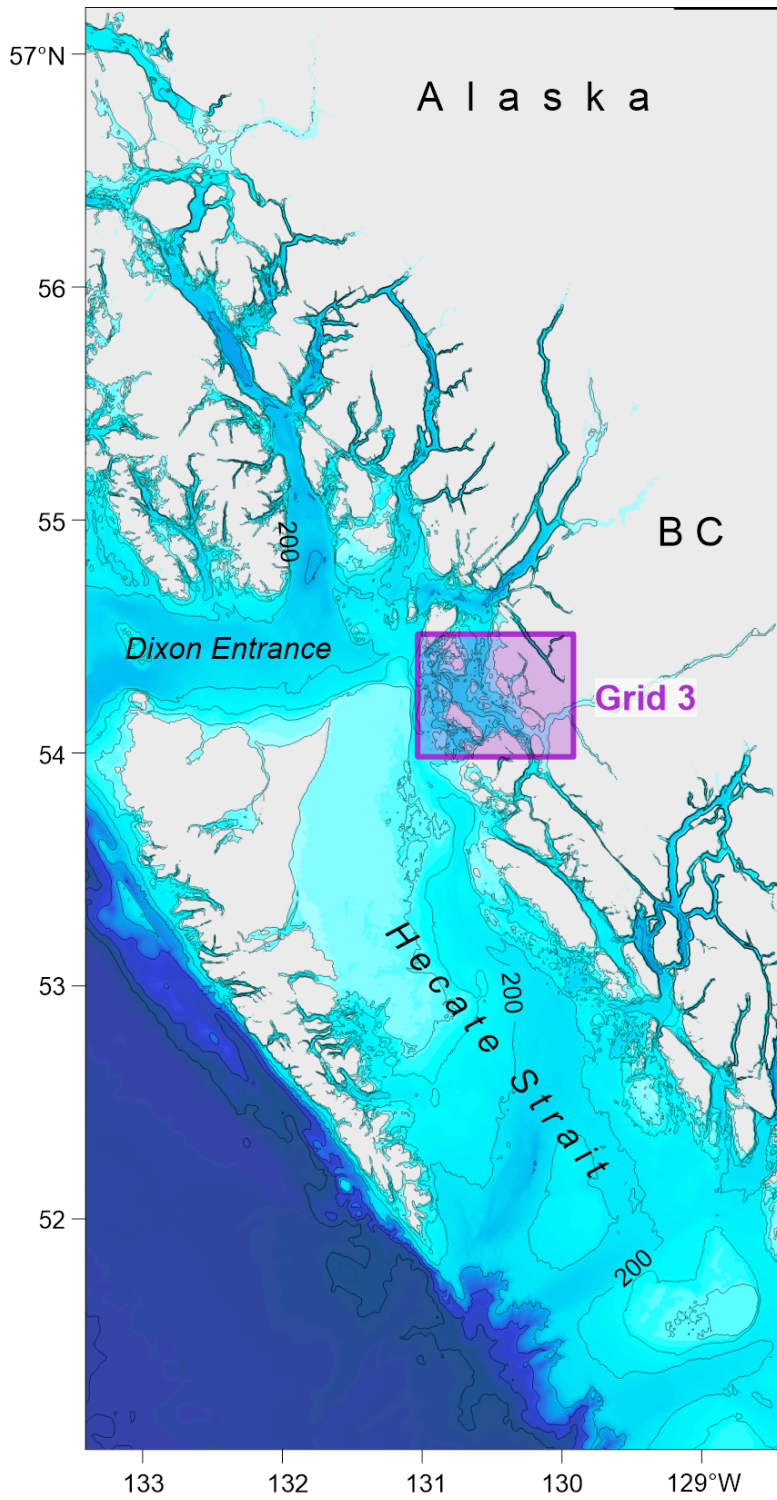


Figure 2.2. The region covered by the medium-scale bathymetric grid (Grid 2) for the northwest coast of British Columbia. The horizontal grid cell scales for this region are approximately 270 m by 280 m. The insert shows the boundaries and location of the second nested grid (Grid 3) covering the region of Prince Rupert and Seal Cove. Depths are in metres (m).

### 2.1.3 Intermediate Grid (Grid 3)

The third numerical grid covers Chatham Sound, the Prince Rupert Harbour waterway and surrounding passes and inlets (Figure 2.3). This grid is of considerable importance since it determines the periods, Q-factor (attenuation rate) and other parameters of the eigen-oscillations set up in the harbour by incoming tsunami waves. Model grid cells were created using the 50-m pre-gridded CHS data provided as part of this study. The gridded data were subsequently re-interpolated from the original local UTM projection to a geographical coordinate system (NAD83 standard) with a rectangular grid cell size of 3 arc-seconds by 1.8 arc-seconds (approximately 54 m by 56 m) in the east-west and north-south directions, respectively.

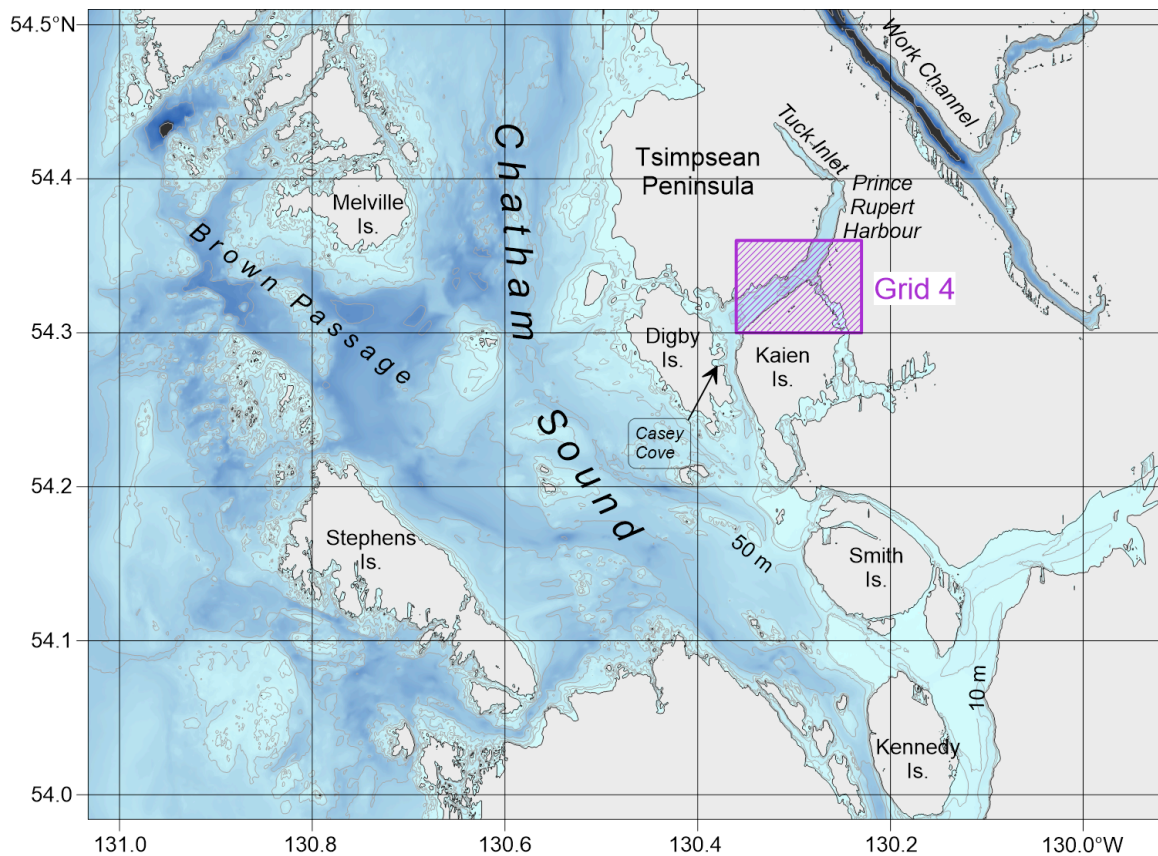


Figure 2.3. Coastal region covered by Grid 3, including Chatham Sound, Brown Passage and Prince Rupert Harbour. The grid scale for this region is approximately 54 m by 56 m. The insert shows the boundaries and location of the third nested grid (Grid 4) covering Seal Cove. Depths are in metres (m).

#### 2.1.4 Final Grid (Grid 4)

The final (fourth) numerical grid has the highest spatial resolution and covers coastal areas near the proposed Coast Guard facilities (Figure 2.4). The grid has been adjusted for the proposed site construction and is designed specifically for estimations of tsunami inundation and tsunami-induced currents in the vicinity of the Coast Guard facilities. A Kriging algorithm (Matheron, 1963) was used to create the grid from the original, irregularly-spaced CHS bathymetric and coastline data. Details on Kriging can be found in Thomson and Emery (2014). The grid (x, y) scale is approximately 11 m by 9 m.

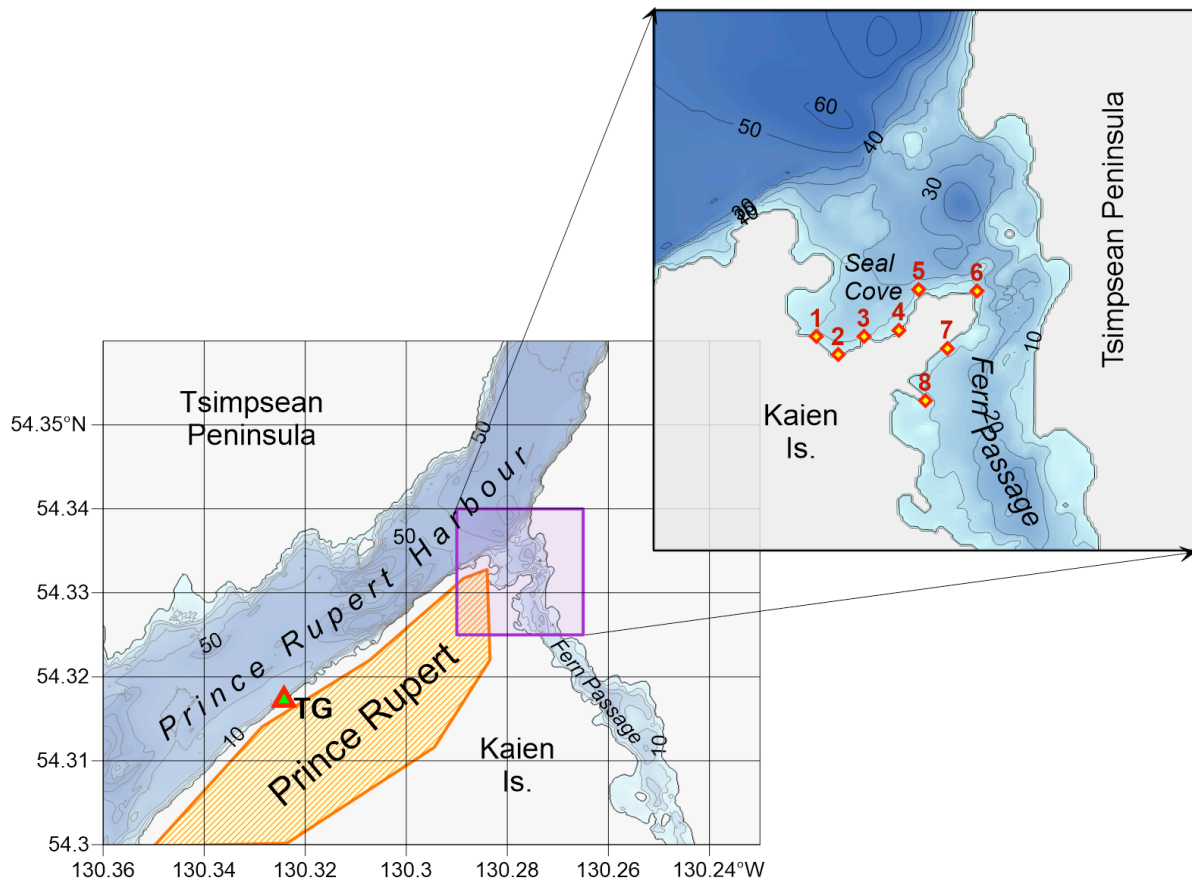


Figure 2.4. The region covered by Grid 4. The fine-scale bathymetric grid has adjusted topography for the region of Prince Rupert and Seal Cove, and has a grid scale of approximately 11 m by 9 m. Also shown are the location of the tide gauge (TG) and the sites at Seal Cove (1-8) for which tsunami wave records have been simulated. Depths are in metres (m).

## 2.2 MODEL REFERENCE LEVELS

Model simulations are generally conducted for tsunami arrival times that coincide with times of mean higher high water (MHHW), as per recommendations for computation of tsunami inundation in the United States (National Tsunami Hazard Mapping Program, 2010; Suleimani et al., 2013). Accordingly, maps of maximum tsunami wave height and current speed presented in this report are referenced to the MHHW mark rather than to the mean tide or to a geodetic reference.

MHHW is used as a reference level for all modelling results. For the Prince Rupert tide gauge, MHHW is 2.32 m above Mean Sea Level (MSL). Similarly, for the Casey Cove tide gauge, located on Digby Island (see Figure 2.3), MHHW is 2.32 m above MSL (Table 2). Based on these measurements, a common reference value of 2.3 m is applied throughout the Prince Rupert region for the tsunami modelling.

Table 2. Chart datum values for stations 9350 and 9354 provided by the CHS. Latitude and longitude are in degrees and minutes. Higher High Water (HHW) is defined in two ways: using all tidal values (Mean) and using only the highest tides (Large).  $Z_0$  is the mean tidal constituent obtained by harmonic analysis of the tidal series.

Tide gauge ID	Name	Latitude (°N)		Longitude (°W)		HHW (m)		MSL (m)
		Deg	Min	Deg	Min	Mean	Large	$Z_0$
9350	Casey Cove	54	16	130	22	6.13	7.34	3.81
9354	Prince Rupert	54	19	130	19	6.16	7.46	3.849

## 2.3 CASCADIA SUBDUCTION ZONE TSUNAMI SOURCE DISTRIBUTIONS

Based on recent advances in Cascadia tsunami source development (cf. Wang and Tréhu, 2016), we considered two different CSZ earthquake source models for tsunamis impacting the coast of British Columbia: Model A, the "buried" model; and Model B, the "splay" model. The models use the same seismic momentum magnitude ( $M_w = 9.0$ ) but two different cross-shore distributions of the associated seismic uplifts. The models have the northward extensions of the Witter et al. (2013) seismic sources off California to Washington, but also include new source areas to the west of Vancouver Island.

The revised models include a contribution of coseismic horizontal displacements to the initial tsunami wave field through a component of ocean surface uplift due to the horizontal motion of the steep

ocean bottom slopes. Numerical tsunami simulations reveal that including the deformation due to horizontal displacements in the source function results in an increase in the far-field tsunami amplitudes. The resulting coseismic vertical deformations are shown in Figure 2.5.

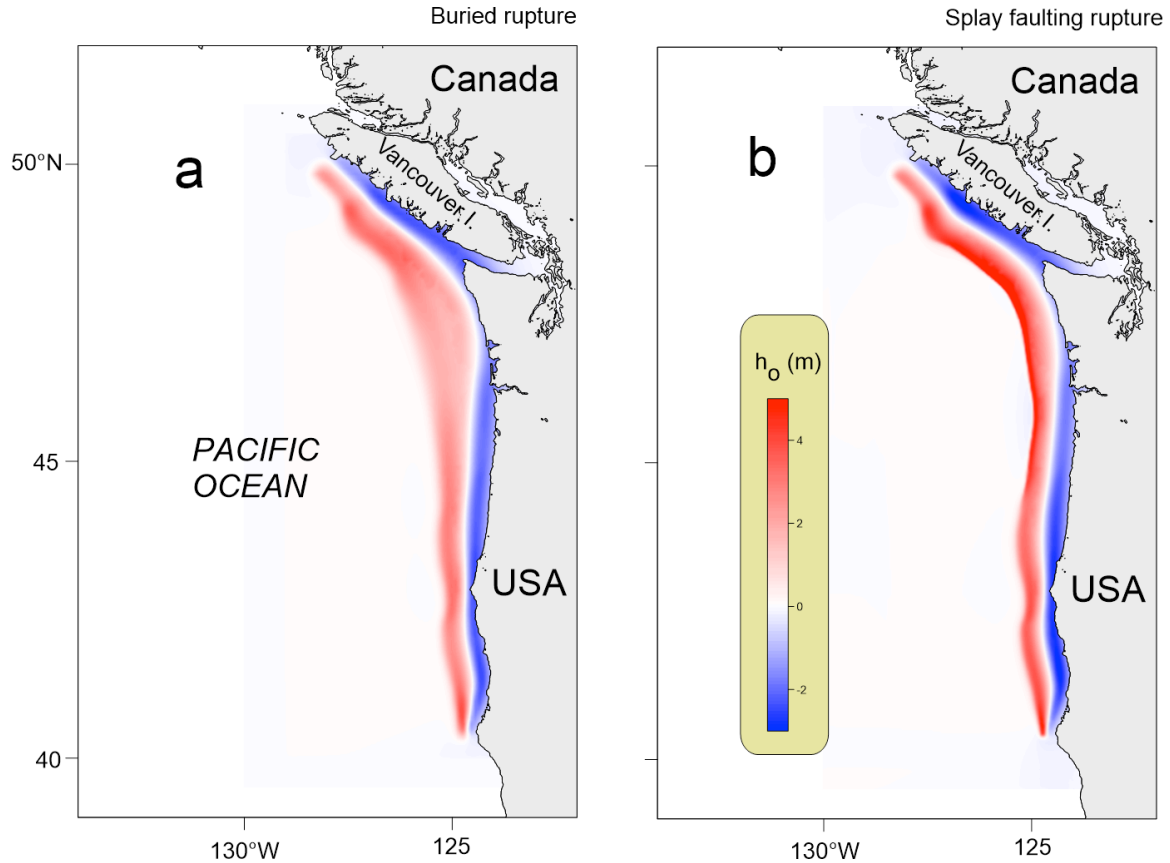


Figure 2.5. Maps of the Cascadia rupture zone tsunami sources according to Gao (2016).  
 (a) Model A: Whole margin buried rupture; and  
 (b) Model B: Whole margin splay-faulting rupture.

Model A is the case when the source deformation slip is located well below the sea bed, whereby the seafloor uplift has a smooth and gentle cross-shore profile, with maximum uplift of 4 m. Model B corresponds to the "splay" model, where the rupture edges are on the surface of the seabed. Maximum uplift is near 8 m. This model corresponds to the case "M1" in the Witter et al. (2013) classification and is considered the most probable scenario. Two previous models for Cascadia tsunami sources for the British Columbia coast used tsunami sources that are somewhere between Models A and B (Cherniawsky et al., 2007; AECOM, 2013).

This page is left intentionally blank



### 3 RESULTS

#### 3.1 COMPARISON OF MODELLED TSUNAMI WAVES FOR TWO CASCADIA SUBDUCTION ZONE SCENARIOS FOR COARSE AND INTERMEDIATE GRIDS

Low-resolution results for CSZ tsunami simulations for Model A and Model B are presented in Figure 3.1. The simulated maps of the tsunami height maxima for the open ocean are quite different. Model B produces much more intensive waves, with stronger interference of waves arriving from the northern and southern sectors of the CSZ. Waves generated by this model using the splay faulting rupture have a stronger impact on coastal areas of Vancouver Island and the US west coast than waves generated by Model A using the buried rupture source model. However, the effect on the area of interest, in Hecate Strait is much less intense in both models, with estimated wave heights of less than one metre.

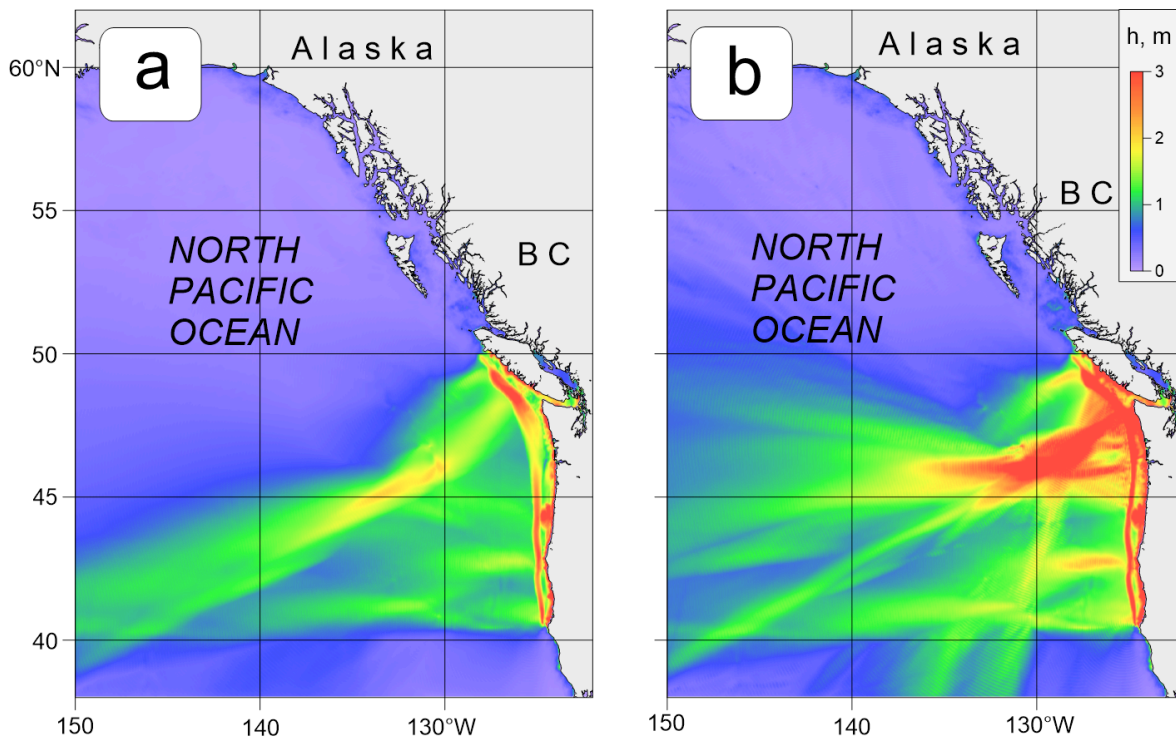


Figure 3.1. Spatial distribution of maximum tsunami wave heights ( $h$ , in metres) for Grid 1 of the nested-grid model for waves associated with the CSZ tsunami for (a) Model A; and (b) Model B.



Grid 2, Figure 3.2 shows details for the northern British Columbia coast around Prince Rupert and Seal Cove. In this region, the predicted tsunami wave heights are all between 0 to 1 m for both models, as noted for Grid 1. In general, Model B provides higher wave amplitudes than Model A, but not for all regions. In essence, northern BC experiences only "side" effects from CSZ tsunamis.

The corresponding detailed results for Chatham Sound and surrounding inlets are shown in Figure 3.3. In eastern Chatham Sound and Prince Rupert Inlet, tsunami waves are slightly higher for Model A than for Model B. The opposite is true in the south-western part of the grid; waves are higher for the case of Model B.

The different tsunami generation responses for Model A and Model B are attributed to differences in the shapes of the tsunami sources: Model A has a smoother shape, while Model B has a sharper shape and higher uplift (Figure 2.5). Accordingly, Model B produces more energy in the high frequency range and less energy in the low frequency range than Model A. For exposed near-field regions, such as the west coast of Vancouver Island and west coast of the USA, the high frequency tsunami waves from Model B produce much higher waves at the coast because of higher amplification as the waves propagate onshore. However, in more protected areas such as Hecate Strait, the differences in wave heights between models is less pronounced, and in some places can be the opposite to that along the outer coast (see Figure 3.3).

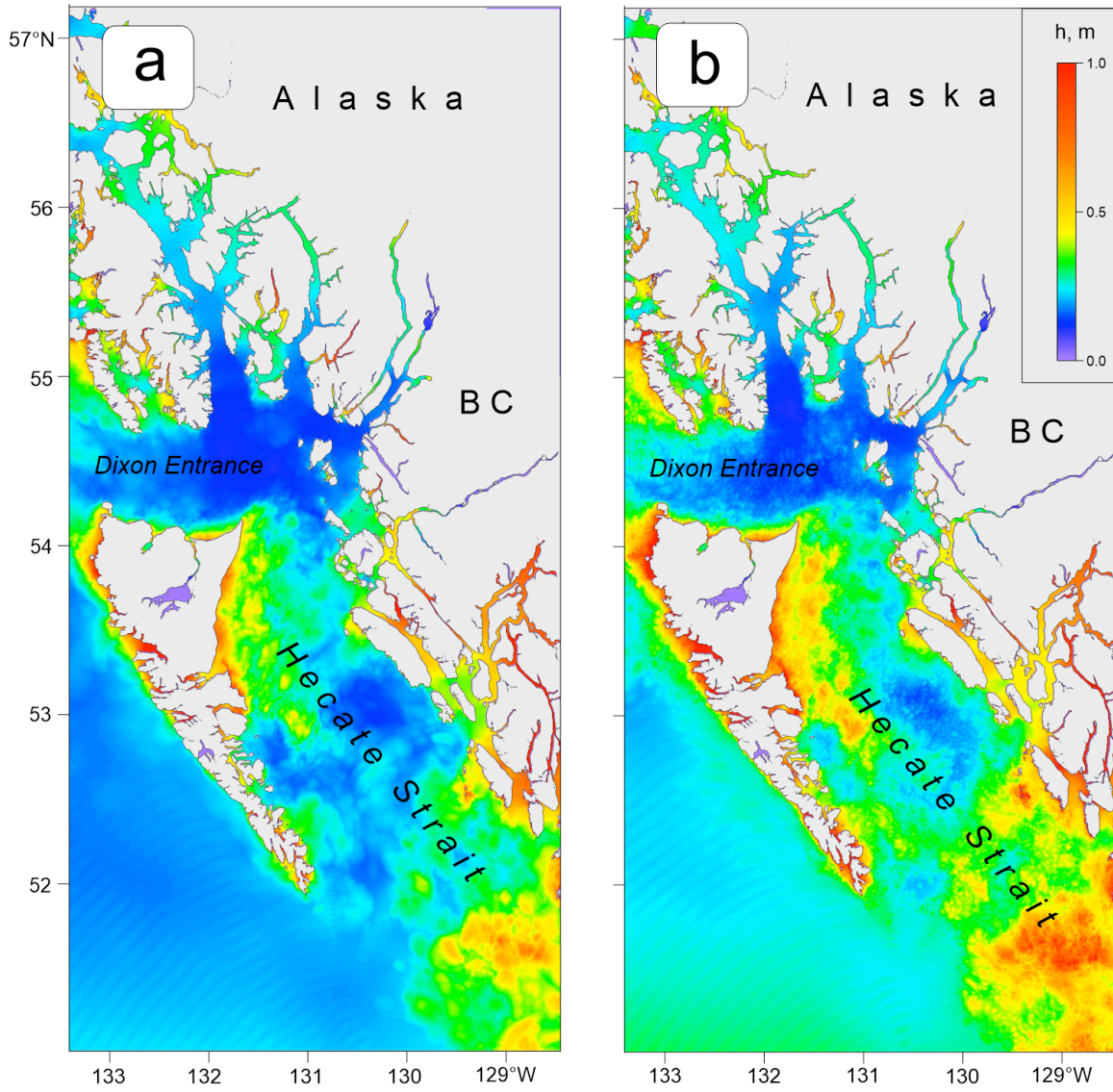
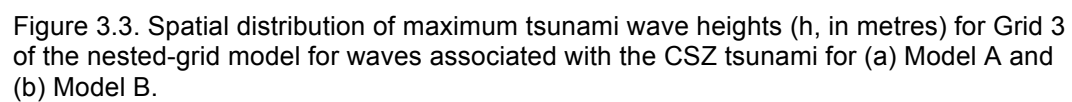


Figure 3.2. Spatial distribution of maximum tsunami wave heights ( $h$ , in metres) for Grid 2 of the nested-grid model for waves associated with the CSZ tsunami for (a) Model A; and (b) Model B.



### 3.2 DETAILED RESULTS FOR SEAL COVE: VARIATIONS IN SEA LEVEL AND TSUNAMI-INDUCED CURRENTS

Detailed distributions of the maximum wave heights and wave-induced currents in Seal Cove and surrounding areas are presented in Figures 3.4 to 3.5. According to Figures 3.4a and 3.4b, the average maximum tsunami height in Seal Cove is about 0.75 m for Model A, and about 0.65 m for Model B. The height distributions are quite similar for both cases, but wave heights for Model B are 15% smaller than those for Model A. Inside Seal Cove, tsunami heights are nearly uniform and close to the values in neighbouring Prince Rupert Harbour. The waves become smaller inside Fern Passage, with wave amplitudes decreasing as they propagate through each narrow part of the channel.

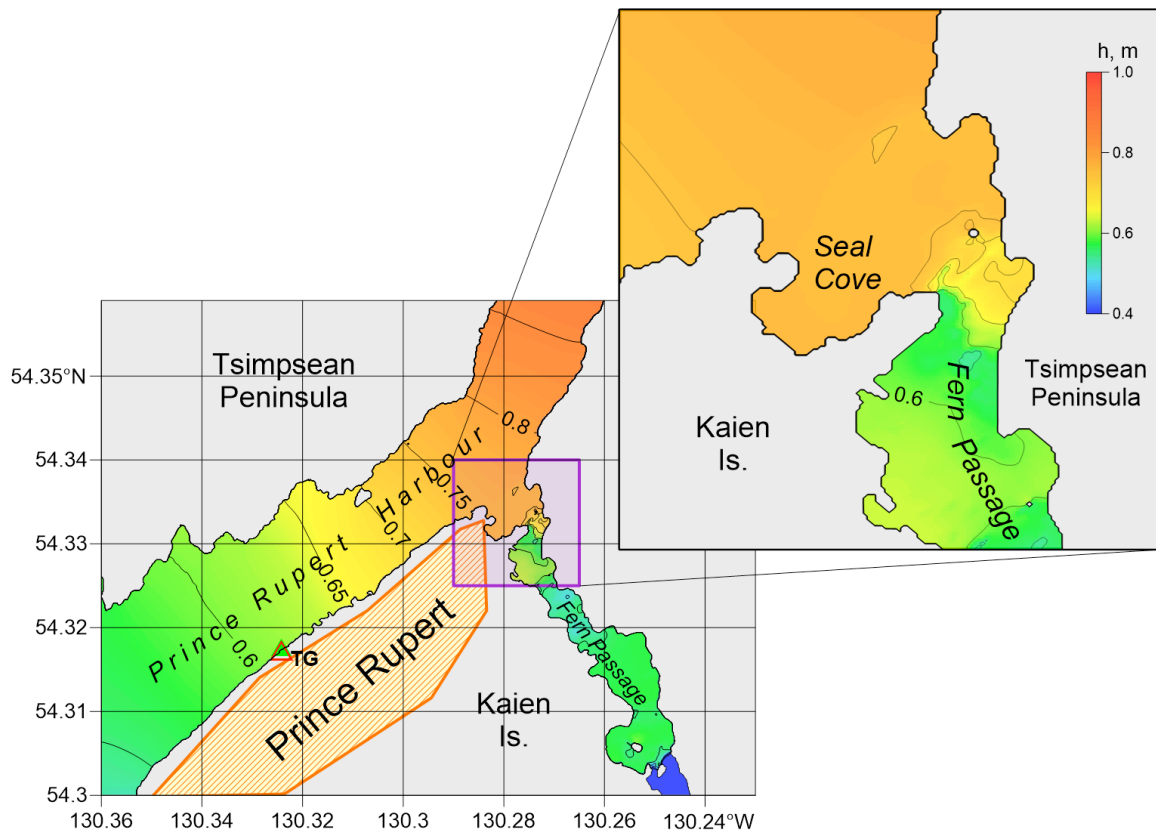


Figure 3.4a. Model A: Distribution of maximum tsunami wave heights ( $h$ , metres) for Grid 4 of the nested-grid model for waves associated with a CSZ tsunami. The insert shows an enlarged segment of the Seal Cove area.

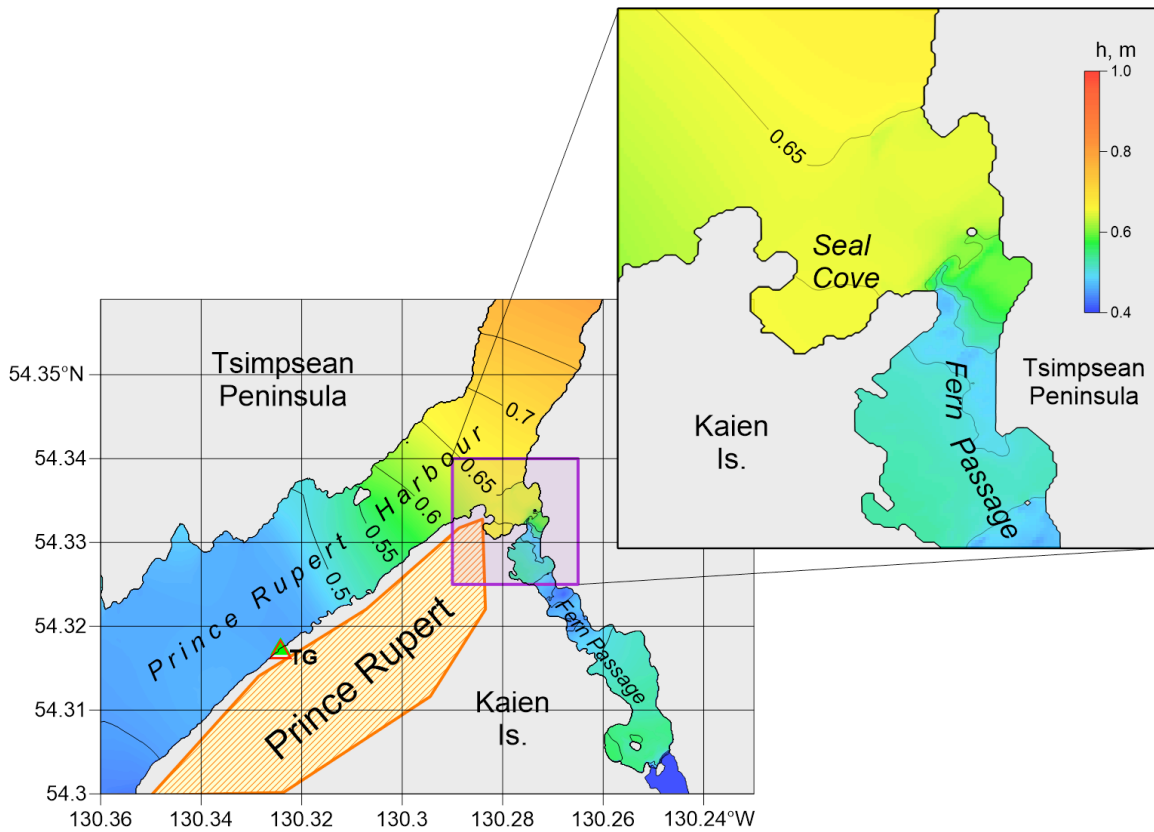


Figure 3.4b. Model B: Distribution of maximum tsunami wave heights ( $h$ , metres) for Grid 4 of the nested-grid model for waves associated with a CSZ tsunami. The insert shows an enlarged segment of the Seal Cove area.

The tsunami-induced currents are weak in Seal Cove for the two cases (Figures 3.5a and 3.5b). Much stronger currents are found for Fern Passage. As with wave height, currents are stronger for Model A whilst the distributions of the currents for both models are similar.

Time series of the modelled waves and wave-induced currents at specific sites are presented in Figures 3.6 to 3.11; the statistical characteristics of these records are found in Tables 3.1, 3.2 and 3.3. It is apparent that the wave heights are nearly identical for sites 1 to 4 with the first crest heights of 0.29 m to 0.26 m and the largest wave heights reaching 0.76 m and 0.65 m for both A and B model simulations, respectively.

At Sites 5 to 8, the first crest height values are similar to Sites 1 to 4, with heights of 0.26 m to 0.29 m at all sites. However, the maximum wave height simulations from A and B are noticeably smaller at Sites 6 to 8, differing by up to 0.25 m (approximately 30 %). At Sites 6 to 8 Model A results range from 0.58 m to 0.63 m and Model B results range from 0.5 m to 0.53 m.

The first wave reaches the Seal Cove region 3.5 hours after the earthquake and is expected to be quite small (less than 0.3 m). The highest wave (roughly 0.7-0.8 m), the sixth wave crest, arrives at Seal Cove 12 hours after the earthquake. Typical tsunami wave periods are about 100 minutes for both models.

Wave-induced currents for sites 1 to 4 are weak (below 0.12 m/s) but become much stronger at sites 5 to 8. Strongest currents occur at Site 6 (1.65 m/s for Model A and 1.53 m/s for Model B) located at Fern Passage.

According to our numerical tsunami modelling, waves generated by a mega-thrust earthquake along the CSZ will be weak in the Seal Cove area. This result is not unexpected given that the area is not directly exposed to CSZ tsunamis and is subject only to side effects arising from the northern edge of the tsunami source region.

**Table 3.1.** Model A simulated tsunami wave parameters for a Cascadia Subduction Zone tsunami at Seal Cove. See Figure 2.4 for the site locations. Travel times for the maximum waves are in hours and minutes (HH:MM) after the start of the earthquake.

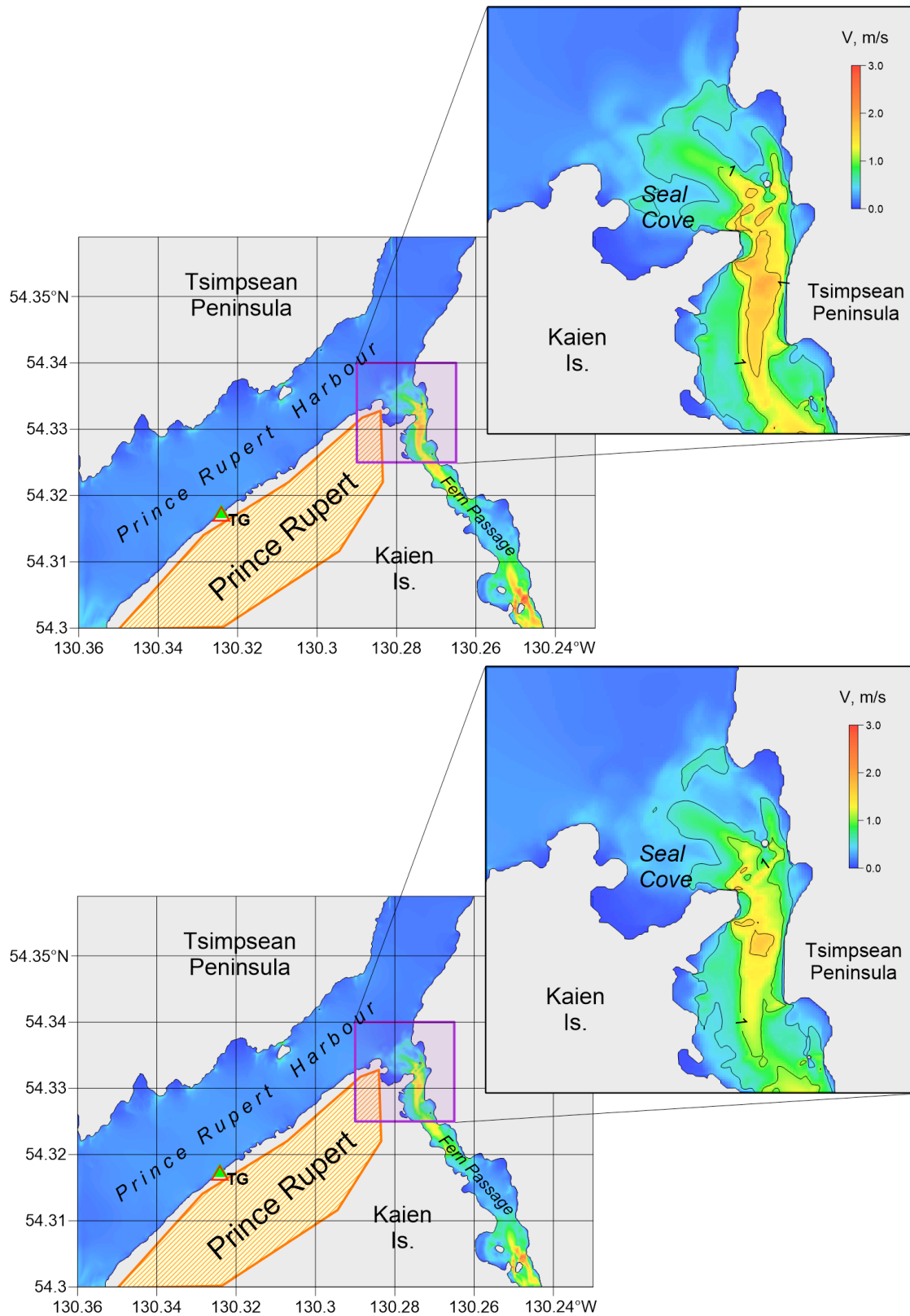
Site No	First crest		Highest crest		Deepest trough	
	Height (m)	Travel time HH:MM	Height (m)	Travel time HH:MM	Height (m)	Travel time HH:MM
1	0.29	03:52	0.76	11:54	-0.73	12:12
2	0.29	03:52	0.76	11:54	-0.73	12:12
3	0.29	03:52	0.76	11:54	-0.73	12:12
4	0.29	03:52	0.76	11:54	-0.73	12:12
5	0.29	03:53	0.76	11:54	-0.74	12:12
6	0.29	03:53	0.63	11:55	-0.74	12:13
7	0.29	03:53	0.58	11:54	-0.60	12:15
8	0.29	03:53	0.61	11:55	-0.60	12:15

**Table 3.2.** Model B simulated tsunami wave parameters for a Cascadia Subduction Zone tsunami at Seal Cove. See Figure 2.4 for the site locations. Travel times for the maximum waves are in hours and minutes (HH:MM) after the start of the earthquake.

Site No	First crest		Highest crest		Deepest trough	
	Height (m)	Travel time HH:MM	Height (m)	Travel time HH:MM	Height (m)	Travel time HH:MM
<b>1</b>	0.26	03:53	0.65	11:58	-0.61	12:11
<b>2</b>	0.26	03:53	0.65	11:58	-0.61	12:11
<b>3</b>	0.26	03:53	0.65	11:58	-0.61	12:11
<b>4</b>	0.26	03:53	0.65	11:58	-0.61	12:11
<b>5</b>	0.26	03:53	0.65	11:58	-0.61	12:11
<b>6</b>	0.26	03:54	0.53	11:58	-0.63	12:12
<b>7</b>	0.26	03:54	0.50	11:58	-0.49	12:12
<b>8</b>	0.26	03:54	0.52	11:58	-0.49	12:12

**Table 3.3.** Models A and B simulations for wave-induced current speeds (V) for a Cascadia Subduction Zone tsunami at Seal Cove. See Figure 2.4 for the site locations. The times for the occurrence of maximum wave-induced currents are in hours and minutes (HH:MM) after the start of the earthquake.

Site No	Model A		Model B	
	Maximum current speed (m/s)	Time of maximum current speed HH:MM	Maximum current speed (m/s)	Time of maximum current speed HH:MM
<b>1</b>	0.03	08:02	0.02	07:13
<b>2</b>	0.01	07:26	0.00	07:57
<b>3</b>	0.12	07:03	0.09	07:17
<b>4</b>	0.03	06:56	0.01	07:10
<b>5</b>	0.73	12:53	0.65	12:50
<b>6</b>	1.65	07:03	1.53	11:34
<b>7</b>	0.40	12:10	0.36	12:12
<b>8</b>	0.61	11:40	0.63	11:44





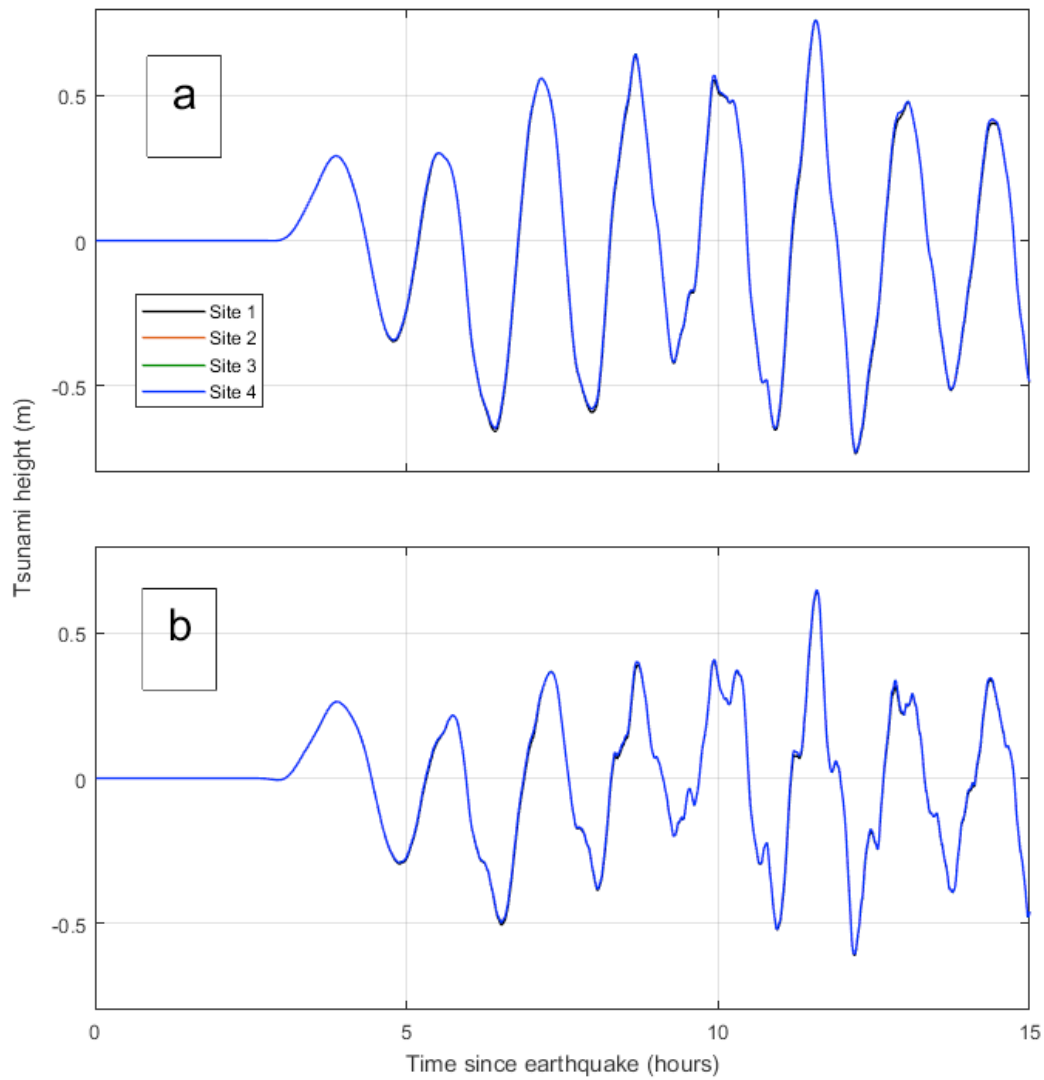


Figure 3.6. (a) Model A; and (b) Model B: Simulated records of water level variations for a CSZ tsunami at Seal Cove for Sites 1 to 4 (See Figure 2.4 for the site locations). Only the records for Site 4 are presented, as those for the other three sites are almost identical.

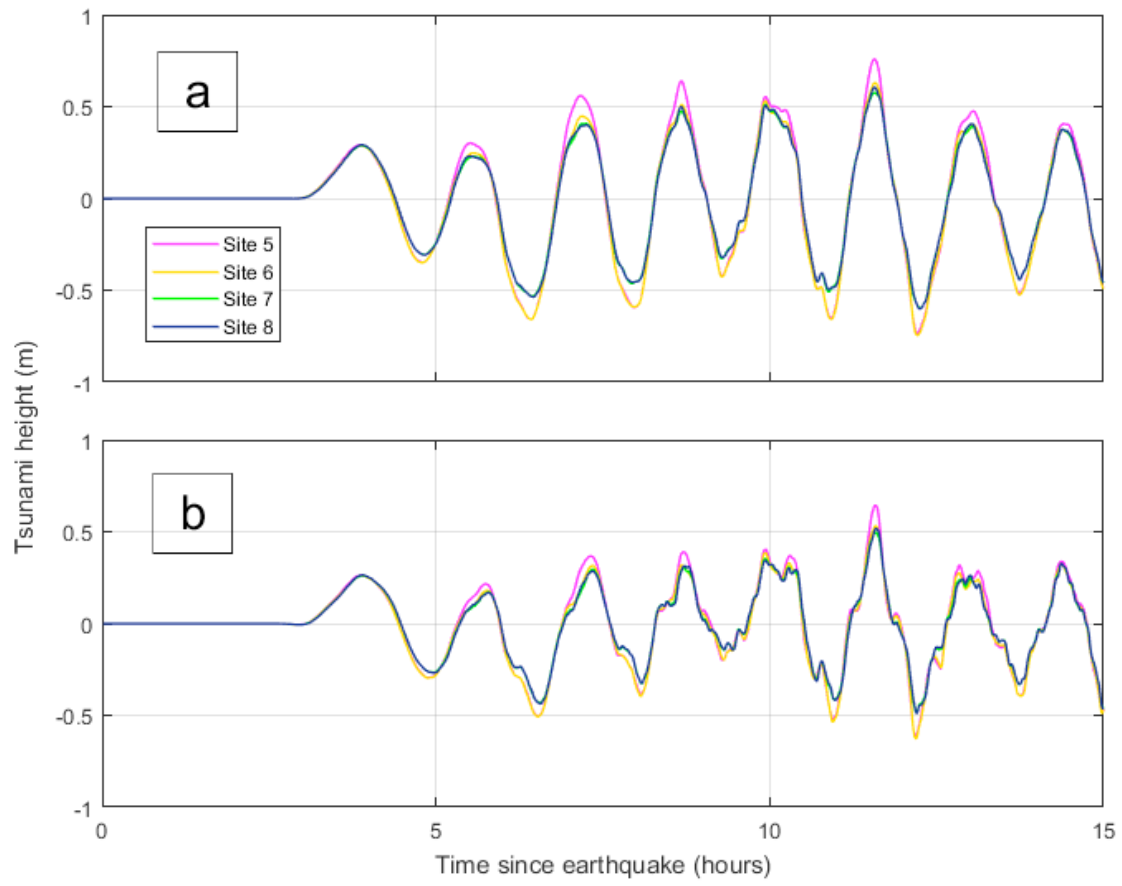


Figure 3.7. (a) Model A; and (b) Model B: Simulated records of water level variations for a CSZ tsunami at Seal Cove for Sites 5, 6, 7 and 8 (See Figure 2.4 for the site locations).

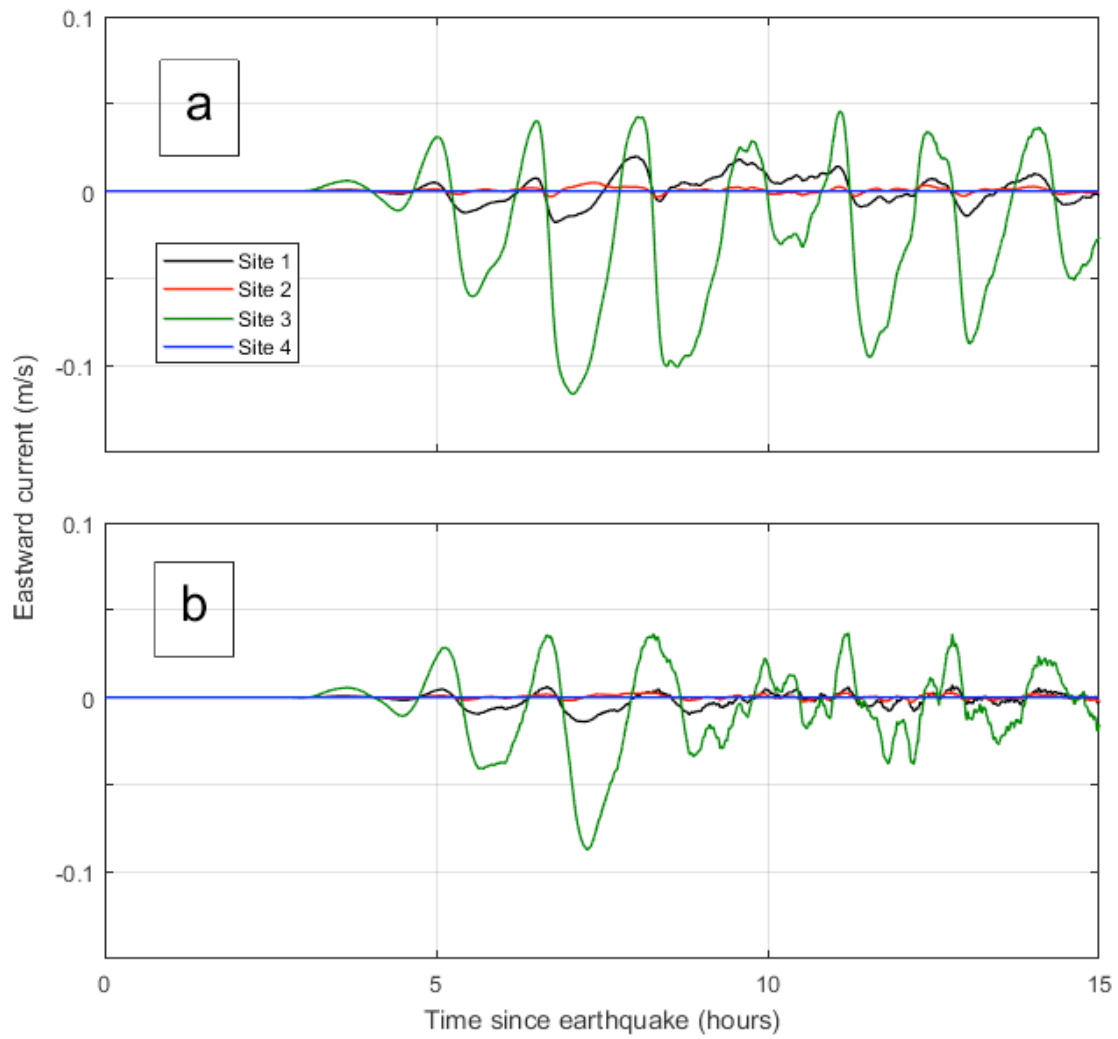


Figure 3.8. (a) Model A; and (b) Model B: Simulated records of the eastward component of current velocity for a CSZ tsunami at Seal Cove for Sites 1, 2, 3 and 4 (See Figure 2.4 for the site locations).

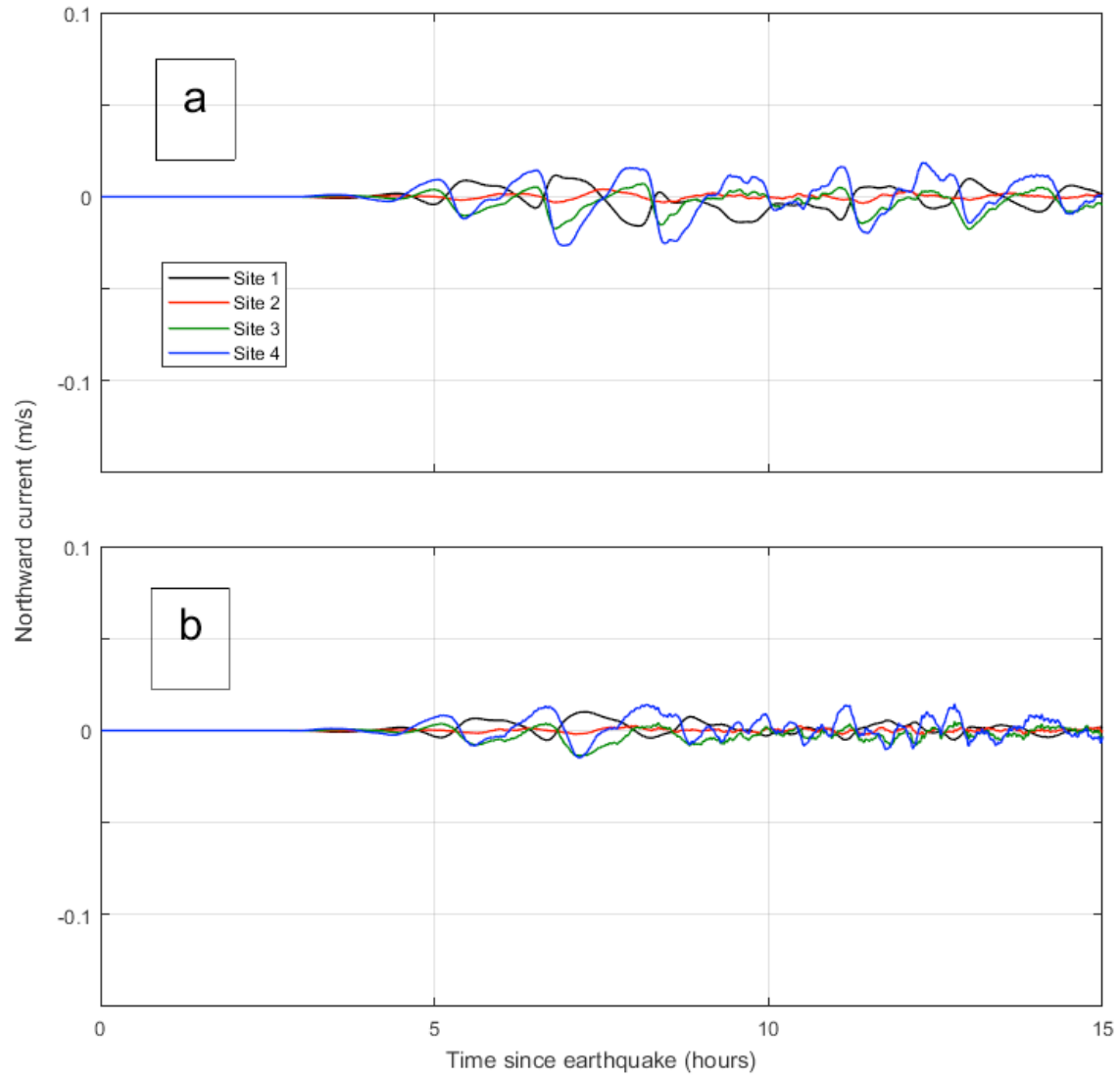


Figure 3.9. (a) Model A; and (b) Model B: Simulated records of the northward component of current velocity for a CSZ tsunami at Seal Cove for Sites 1, 2, 3 and 4 (See Figure 2.4 for the site locations).

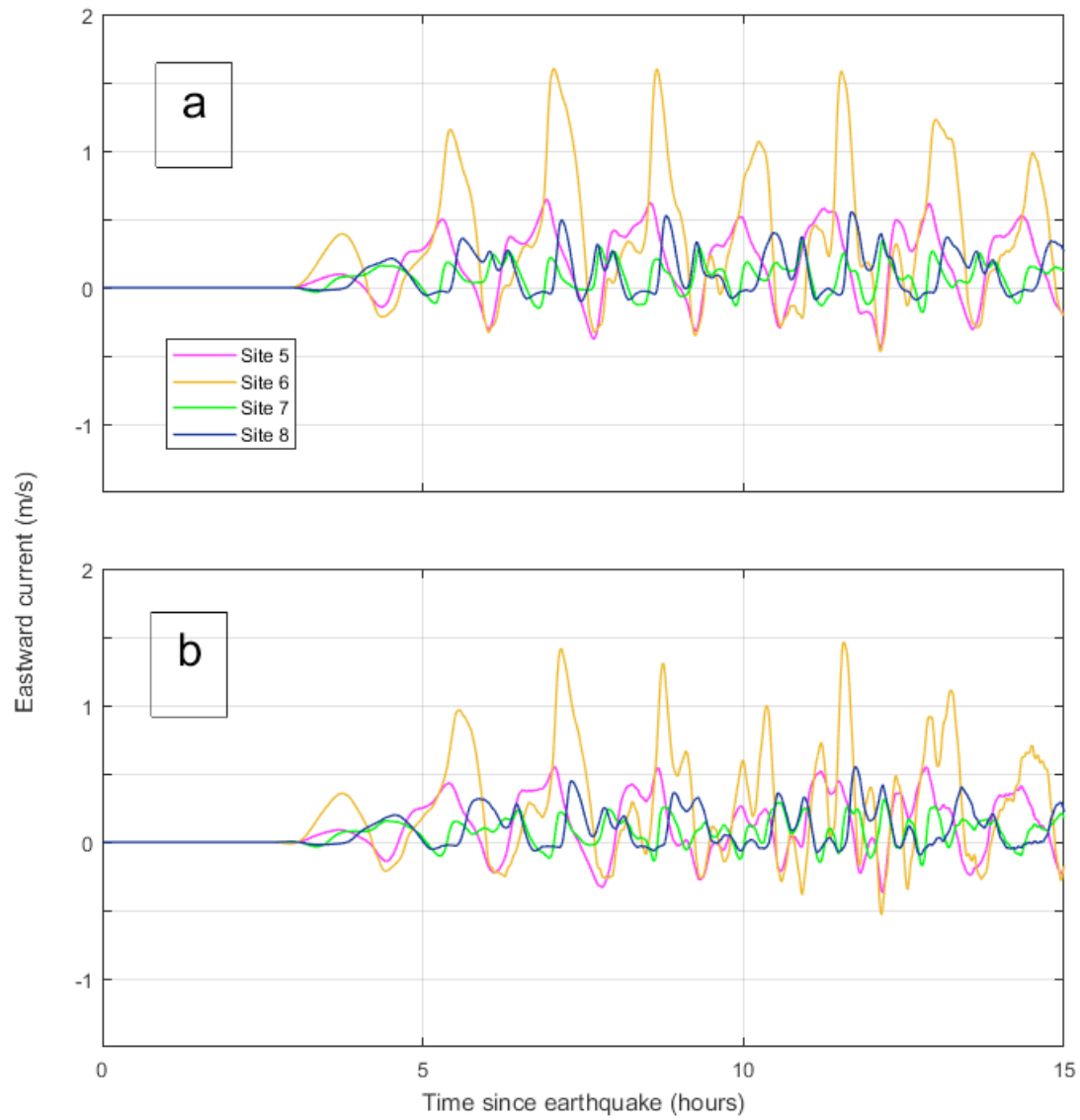


Figure 3.10. (a) Model A; and (b) Model B: Simulated records of the eastward component of current velocity for a CSZ tsunami at Seal Cove for Sites 5, 6, 7 and 8 (See Figure 2.4 for the site locations).

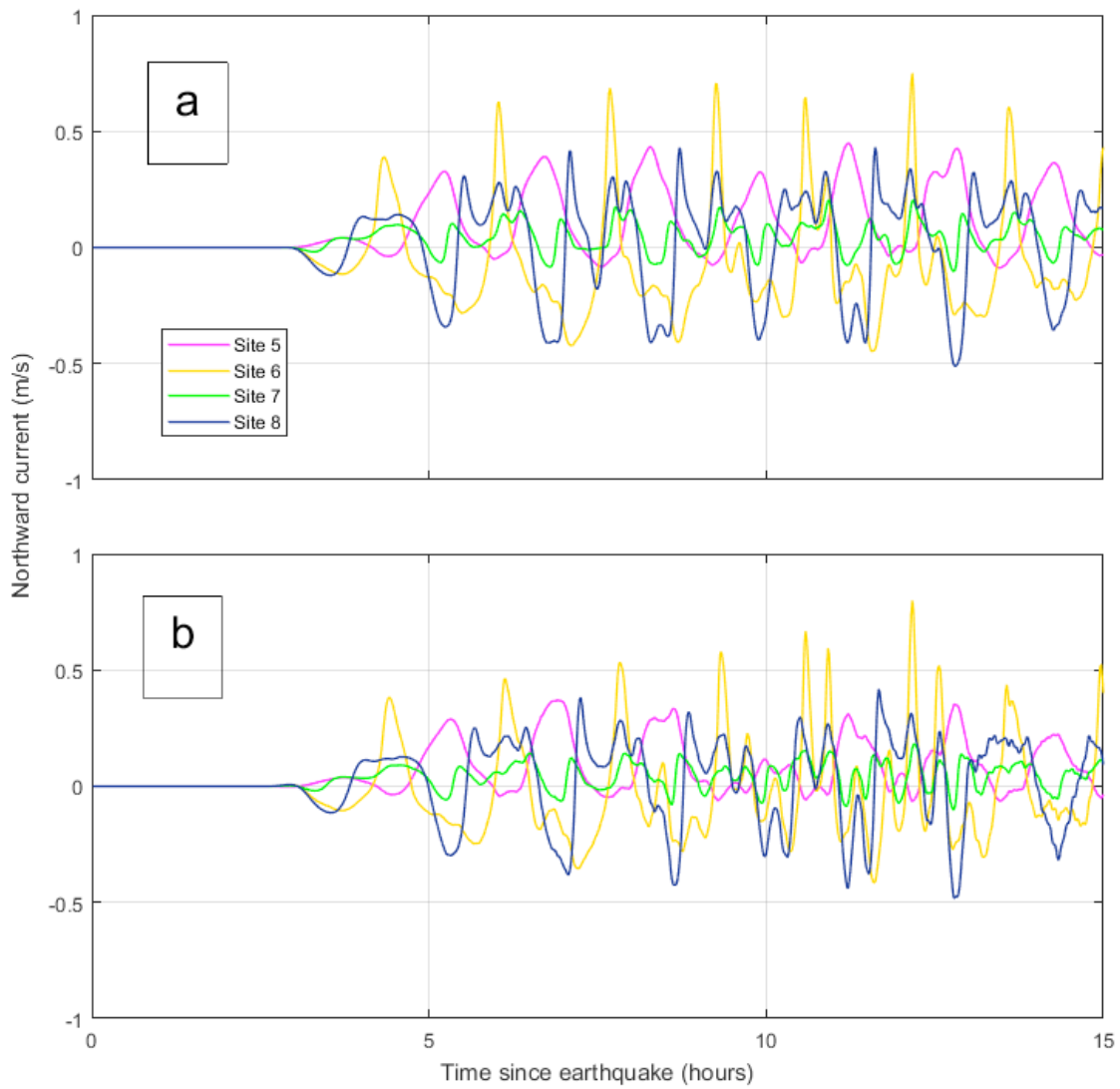


Figure 3.11. (a) Model A; and (b) Model B: Simulated records of the northward component of current velocity for a CSZ tsunami at Seal Cove for Sites 5, 6, 7 and 8 (See Figure 2.4 for the site locations).

This page is left intentionally blank

## 4 CONCLUSIONS

A high-resolution, nested-grid tsunami model was used to simulate tsunami waves and wave-induced currents that will be generated in Seal Cove by a Cascadia Subduction Zone (CSZ) earthquake. Two versions of the earthquake and tsunami source region were used: Model A, a whole margin buried rupture; and Model B, a whole margin splay-faulting rupture. The main results of the numerical modelling for the Seal Cove area are:

- The whole margin buried rupture scenario (Model A) produced higher waves in the Seal Cove area than the whole margin splay-faulting rupture scenario (Model B);
- The maximum wave heights in Seal Cove will be 0.76 m (Model A case) and 0.65 m (Model B case) above the tidal level at the time of the event; the 6-th wave will be the highest wave;
- Tsunami wave periods will range from 70 to 105 minutes;
- Tsunami wave amplitudes will be nearly uniform throughout Seal Cove;
- Tsunami-induced currents in Seal Cove will be weak;
- Tsunami-induced currents in neighbouring Fern Passage will be quite strong and reach speeds of around 2 m/s (4 knots);

Because many of the details of future possible tsunamis remain unknown, we recommend applying a safety factor of 50%, which should be added to the estimated tsunami amplitudes for a CSZ tsunami event. In particular, the safety level for Seal Cove should be 1.14 m above Mean Higher High Water, or 3.45 m above Mean Sea Level. This level, which specifically applies to a magnitude 9.0, CSZ tsunami is below the recorded extreme high-water mark for the region.

More detailed predictions on the landward extent of tsunami wave run-up and inundation in the Seal Cove region will require more advanced numerical simulations, which permit wetting and drying of the land. The model should be able work with strong nonlinearity and friction and incorporate discontinuities between wet and dry domains. Such studies will require detailed coastal elevation data and Lidar bathymetry along the shoreline. Future model upgrades should also take into account new advances in CSZ earthquake source regions developed by geophysicists.



This page is left intentionally blank

## **5 ACKNOWLEDGEMENTS**

The authors gratefully thank Peter Wills and Denny Sinnott of the Canadian Hydrographic Service for providing the bathymetric data and tide gauge records for this study. Alexander Rabinovich and Maxim Krassovski of the Institute of Ocean Sciences, for assisting with the data processing and numerical grid formulation, and Kelin Wang of the Geological Survey of Canada, Natural Resources Canada for providing us his latest source models for the Cascadia earthquake and tsunامي. Lastly, we thank Alison Scoon for helping transform the original report into a formal technical report.

This page is left intentionally blank

## 6 REFERENCES

- AECOM (2013). Modelling of Potential Tsunami Inundation Limits and Run-Up, Capital Regional District, Project No. 6024 2933, 36 p.
- Atwater, B.F. et al. (1995), Summary of coastal geologic evidence for past great earthquakes at the Cascadia Subduction Zone, *Earthquake Spectra*, 11 (1), 1-18.
- Becker, J. J., D. T. Sandwell, W. H. F. Smith, J. Braud, B. Binder, J. Depner, D. Fabre, J. Factor, S. Ingalls, S-H. Kim, R. Ladner, K. Marks, S. Nelson, A. Pharaoh, R. Trimmer, J. Von Rosenberg, G. Wallace, P. Weatherall. (2009), Global Bathymetry and Elevation Data at 30 Arc Seconds Resolution: SRTM30\_PLUS, *Marine Geodesy*, 32:4, 355-371, DOI: 10.1080/01490410903297766.
- Cherniawsky, J.Y., Titov, V.V., Wang, K., and Li, J.-Y. (2007), Numerical simulations of tsunami waves and currents for southern Vancouver Island from a Cascadia megathrust earthquake, *Pure Appl. Geophys.* 164 (2-3), 465-492, doi:10.1007/s00024-006-0169-0.
- Cheung, K.F., Wei, Y., Yamazaki, Y., and Yim, S.C.S. (2011), Modeling of 500-year tsunamis for probabilistic design of coastal infrastructure in the Pacific Northwest, *Coastal Engineering* 58 (2011) 970–985
- Clague, J.J., Bobrowsky, P.T., and Hutchinson, I. (2000), A review of geological records of large tsunamis at Vancouver Island, British Columbia, and implications for hazard, *Quatern. Science Rev.*, 19, 849-863.
- Clague, J.J., Munro, A., and Murty, T.S. (2003), Tsunami hazard and risk in Canada, *Natural Hazards* 28 (2-3), 433-461.
- Dragert, H., and Rogers, G.C. (1988), Could a megathrust earthquake strike southern British Columbia? *GEOS*, 17 (3), 5-8.
- Fine, I.V., Cherniawsky, J.Y., Rabinovich, A.B., and Stephenson, F.E. (2008), Numerical modeling and observations of tsunami waves in Alberni Inlet and Barkley Sound, British Columbia, *Pure Appl. Geophys.*, 2008, 165, (11/12), 2019-2044.
- Gao, D. 2016. Defining Megathrust Tsunami Sources at Northernmost Cascadia Using Thermal and Structural Information. Master of Science Thesis, School of Earth and Ocean Sciences, The University of Victoria, <https://dspace.library.uvic.ca/handle/1828/7435>.
- Leonard, L.J., Rogers, G.C. and Mazzotti, S. (2014). Tsunami hazard assessment of Canada, *Natural Hazards*, 70, 237-274.

- Myers, E.P., Baptista, A.M., and Priest, G.R. (1999), Finite element modelling of potential Cascadia subduction zone tsunamis, *Sci. Tsunami Hazards*, 17, 3–18.
- Ng, M.K.-F., LeBlond, P.H., and Murty, T.S. (1990), Numerical simulation of tsunami amplitudes on the coast of British Columbia due to local earthquakes, *Sci. Tsunami Hazards* 8, 97-127.
- Suleimani, E.N., Nicolsky, D.J., and Koehler, R.D. (2013). Tsunami Inundation Maps of Sitka, Alaska. Report of Investigations 2013-3, State of Alaska, Department of Natural Resources, Division of Geological and Geophysical Surveys, Fairbanks, AK, 76 p., 1 sheet, scale 1:250,000. doi: 10.14509/26671.
- Satake, K., Shimazaki, K., Tsuji, K., and Ueda, K. (1996), Time and size of a giant earthquake in Cascadia earthquake inferred from Japanese tsunami records of January 1700, *Nature* 379, 246–249.
- Thomson, R. E. and Emery, W. J. (2014). *Data Analysis Methods in Physical Oceanography*: 3<sup>rd</sup> Edition. Elsevier Science, Amsterdam, London, New York (August 2014), 716 p.
- Wang, K., and Tréhu, A.M. (2016), Invited review paper: Some outstanding issues in the study of great megathrust earthquakes—The Cascadia example, *J. Geodynamics*, 98, 1-18.
- Whitmore, P.M. (1993), Expected tsunami amplitudes and currents along the North American coast for Cascadia Subduction Zone earthquakes, *Natural Hazards* 8, 59–73.
- Witter, R.C., Zhang, Y.J., Wang, K., Priest, G.R., Goldfinger, C., Stimely, L., English, J.T., and Ferro, P.A. (2013), Simulated tsunami inundation for a range of Cascadia megathrust earthquake scenarios at Bandon, Oregon, USA, *Geosphere*, 9 (6), 1783-1803, doi: 10.1130/GES00899.1